Chemical Science

ROYAL SOCIETY OF CHEMISTRY

EDGE ARTICLE

View Article Online
View Journal | View Issue

Cite this: *Chem. Sci.*, 2025, **16**, 17876

All publication charges for this article have been paid for by the Royal Society of Chemistry

A new paradigm for valorization of waste poly(glycolic acid): facile coupling with epoxides and synthesis of copolyesters with enhanced performance

Feng Ren,[ab] Zhuangzhuang Liang,[ab] Yifan Jia,[ab] Bokun Li,[ab] Zhiqiang Sun,[a] Chenyang Hu, *[a] Xuan Pang *[ab] and Xuesi Chen [ab]

Poly(glycolic acid) (PGA) is one of the most widely used biodegradable polyesters, but its efficient valorization presents a long-standing challenge. Herein, we report the first facile PGA valorization strategy by utilizing epoxides to upcycle PGA into fused lactones under mild conditions (<100 °C), and subsequent copolymerization to produce copolyesters with wide potential tunability and enhanced performance. In the presence of epoxides and a chromium-based catalyst, PGA was efficiently transformed into fused lactones with a wide range of potential structural adjustability. Subsequently, *via* copolymerization of the obtained lactones and ε-caprolactone (ε-CL), random copolyesters with tunable compositions and high molecular weights (MWs) were obtained. Notably, the copolyesters show a broad range of thermal and mechanical properties, which also overcomes the trade-off in tensile strength and ductility commonly observed for poly(ε-caprolactone) (PCL) or binary copolymers based on ε-CL/other lactones. For example, high MW copolyesters with optimal compositions (P(6-MDO)$_6$-*co*-PCL$_{94}$ and P(6-MDO)$_8$-*co*-PCL$_{92}$) show both superior tensile strength (45.4–46.2 MPa) and ductility (1938–2186%). Apart from excellent mechanical properties and thermal stability, all copolyesters possess good chemical recyclability (>87%), establishing a closed-loop life cycle for a sustainable circular economy. This study offers the first efficient, cost-effective and versatile upcycling route for PGA.

Received 1st August 2025
Accepted 27th August 2025

DOI: 10.1039/d5sc05815e

rsc.li/chemical-science

Introduction

Upcycling of waste commodity plastics is a promising strategy to realize a circular polymer economy. For biodegradable polymers, while the polymer backbones are designed to undergo hydrolysis in the natural environment and can be eventually degraded to CO_2 and H_2O,[1–6] the valuable carbon sources within their repeating units are lost during this process. Moreover, the intermediate degrading products can be potentially hazardous to the ecology.[7] In contrast, chemical (up)cycling presents unique advantages in terms of making the most of pristine polymers by retaining the repeat units and, in turn, producing high-value products. Furthermore, it is highly desirable to valorize the biodegradable polymers into monomers that can be directly reused in polymerizations.

Among biodegradable polymers, aliphatic polyesters hold the largest market share and have attracted considerable attention as sustainable substitutes for petroleum-based polymers.[8–10] As a representative, PGA has exceptional mechanical robustness, gas barrier properties, and biodegradability, making it broadly applicable in biomedicine, food packaging, agricultural films, and other fields.[11–15] Driven by the increasing demand across various industries, PGA's market is projected to reach USD 172 billion by 2025 and USD 954.9 billion by 2033.[16]

Nevertheless, akin to common biodegradable polymers, most PGAs undergo biodegradation to form glycolic acid and eventually lead to CO_2 and H_2O products under specific environmental conditions.[17–20] In contrast, although PGA can be mechanically recycled, this process is usually accompanied by deterioration of polymer properties.[12,21] Therefore, chemical upcycling is one of the most economically efficient and viable methods for PGA at the end of life, which is of particular significance considering the relatively high cost of glycolic acid and glycolide (GA).[22–24] However, compared with other polyesters such as poly(lactic acid) (PLA) and PCL, PGA possesses higher crystallinity and solvent resistance, making its chemical (up)cycling much more difficult.[25–27] As a result, attempts of PGA chemical (up)cycling have thus far met with limited success, as facile and versatile strategies are yet to be developed. Specifically, to our knowledge, the (up)cycling of PGA was only realized

[a]*State Key Laboratory of Polymer Science and Technology, Changchun Institute of Applied Chemistry, Chinese Academy of Sciences, Changchun 130022, China. E-mail: cyhu@ciac.ac.cn; xpang@ciac.ac.cn*

[b]*School of Applied Chemistry and Engineering, University of Science and Technology of China, Hefei 230026, China*

by depolymerizing PGA to GA under rigorous conditions (>200 °C),[28,29] or *via* transesterification, in which γ-butyrolactone (BL) was used as both solvent and comonomer to treat PGA to produce upcycled copolymer of poly(GA-*co*-BL) that can be further recycled to glycolic acid and BL, but the low MW of the obtained poly(GA-*co*-BL) might limit further applications.[30] However, disadvantages of existing PGA (up)cycling routes, including energy-intensiveness and restricted type of products, render this approach uneconomical and lacking in adaptability.

In a prior work, we disclosed that GA can be coupled with epoxides to form six-membered lactones facilitated by the catalytic system of Salen-Cr(III) and bis(triphenylphosphine)-iminium chloride (PPNCl) at 80 °C.[31] During the coupling reaction, GA first underwent ring-opening polymerization to form PGA oligomers, whose chain end was subsequently activated to attack the epoxides to form alkoxy species; and the alkoxy species backbite on the adjacent carbonyl group to eventually form the fused lactones of glycolic acid and epoxides (Scheme S1). Inspired by this work, we envisioned that PGA may be upcycled with epoxides under mild conditions to generate the fused lactones *via* a similar mechanism, which would open up exciting new possibilities for the facile and versatile upcycling of PGA. Furthermore, while the homopolymerization of this new type of lactones was preliminarily studied in our prior report, its modest polymerizability was discovered to result in homopolymers with limited molecular weight (<10 kDa) and inferior material performance. In contrast, these potential PGA-derived monomers may be uniquely suited as comonomers to be polymerized with common lactones and prepare copolyesters with versatile compositions and unique performance.

In the realm of synthesizing copolyesters, research on the copolymerization of ε-CL with other lactones is gathering ever-increasing interest among the scientific community. ε-CL is a popular lactone with ready availability and high polymerizability,[32–34] and PCL can be obtained by the ring-opening polymerization (ROP) of ε-CL as a semicrystalline polymeric material. Owing to its advantages of excellent biodegradability and biocompatibility, PCL also holds promise in biomedical applications.[35–41] However, as there is a trade-off in the mechanical strength and ductility commonly observed for PCL-based materials, their use in many applications is precluded. While copolymerization of ε-CL and other lactones can be a viable strategy to tackle this dilemma, synthesizing copolyesters simultaneously showing high mechanical strength and high ductility *via* binary copolymerization of ε-CL/other lactones represents a longstanding challenge. For example, PLA-*co*-PCL shows modest tensile strength (σ_B ~17.6 MPa) and stretchability (ε_B ~877%),[42] whereas poly(3-hydroxyburtyrate-*co*-ε-caprolactone) (P3HB-*co*-PCL) displays better tensile strength (σ_B ~20.5 MPa) at the expense of stretchability (ε_B ~106%).[43] For PGA-*co*-PCL, both tensile strength and stretchability are significantly undermined (σ_B ~6 MPa, ε_B ~2.7%).[44] In addition, while poly(*p*-dioxanone-*co*-ε-caprolactone) (PDO-*co*-PCL) exhibits good ductility (ε_B ~1700%), it shows much lower strength (σ_B ~10 MPa).[45] Therefore, the discovery of new comonomers that are capable of producing copolyesters together with ε-CL to achieve both enhanced mechanical strength and ductility would be a significant advance.

In this work, we report the first facile PGA upcycling to synthesize fused lactones with epoxides under mild conditions and their copolymerization with ε-CL (Scheme 1). This approach enables versatile modulation of the monomer substitutions by choosing different epoxides. The obtained monomers can be efficiently copolymerized with ε-CL, and a series of high molecular weight copolymers with different compositions can be obtained. The influence of monomer incorporation and monomer substituents on the crystallinity, thermal and mechanical properties of the copolymers was investigated. Besides reporting the first facile and versatile upcycling route of PGA, this work also documents a rare example of novel PCL-based copolymers with both enhanced mechanical strength and ductility, as well as chemical recyclability.

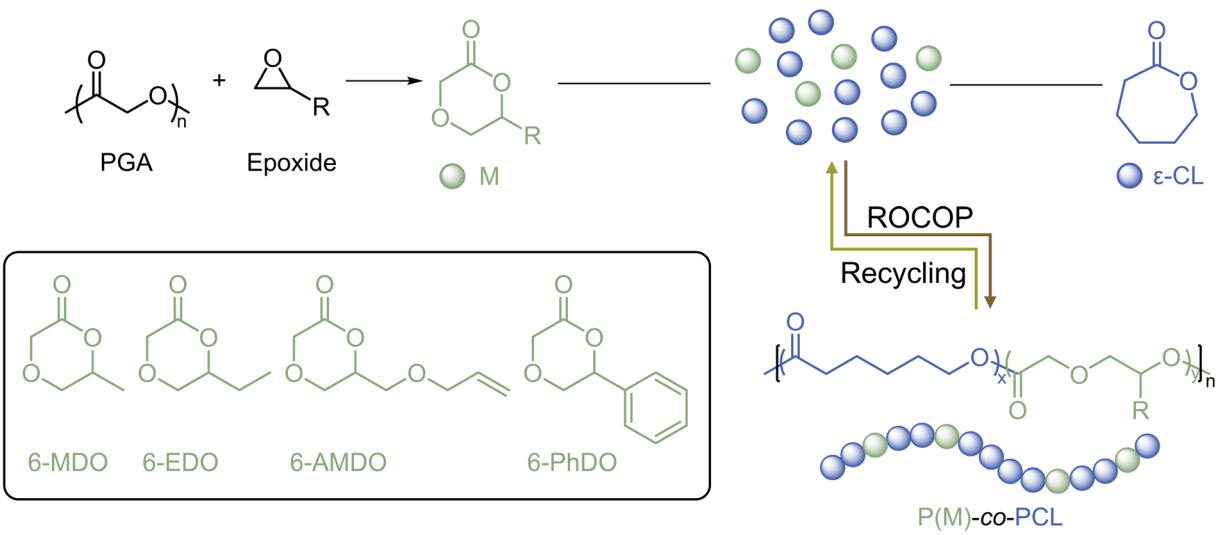

Scheme 1 Synthesis of monomers and copolymerization with ε-CL in one pot.

Results and discussion

Synthesis of fused monomers

At the outset, by adapting the synthetic protocol of fused lactones using GA and epoxides as raw materials,[31] we coupled commercial PGA (industrial grade pellets, MW = 100 kDa) with epoxides in an attempt to obtain the monomers. After running the reaction in the presence of propylene oxide (PO) and catalysts at 80 °C for 3 days ([Salen-Cr(III)]/[PPNCl]/[PGA]/[PO] ratio of 1 : 1 : 100 : 200, catalyst structures shown in Scheme S2), there was almost no visual change on the PGA pellets. The crude mixture was further monitored by ^{1}H NMR, and only polyether was observed with no fused lactone formed. We attributed the much poorer reaction efficiency of PGA compared with GA to the poor solubility of PGA. Moreover, the small surface area of PGA pellets would further handicap their contact with the solvent. Therefore, in order to improve the reaction efficiency of PGA by increasing the contact area, we pretreated the PGA pellets by freezing them in liquid nitrogen and grinding them into powder. Excitingly, by replacing PGA pellets with the obtained PGA powder as the starting material, PGA disappeared after 3 days under the same reaction conditions. Meanwhile, the ^{1}H NMR spectrum of the reaction mixture verified the formation of the fused monomer with satisfactory conversion (71%). It should also be noted that this conversion was still lower than that synthesized from GA feedstock (conversion = 94%) under otherwise similar conditions ([Salen-Cr(III)]/[PPNCl]/[GA]/[PO] ratio of 1 : 1 : 200 : 400, at 80 °C for 3 days). By reacting the PGA powder with different epoxides under similar mild conditions, we successfully obtained a series of six-membered fused lactone monomers with various substituents, *i.e.*, 6-methyl-1,4-dioxan-2-one (6-MDO), 6-ethyl-1,4-dioxan-2-one (6-EDO), 6-((allyloxy)methyl)-1,4-dioxan-2-one (6-AMDO), and 6-phenyl-1,4-dioxan-2-one (6-PhDO), in yields of 56–68%. The successful synthesis of monomers was solidified by ^{1}H NMR, ^{13}C NMR spectroscopy (Fig. S2–S9). To our knowledge, these results not only provide the first effective route for the (up)cycling of PGA under mild conditions (<100 °C), but also facilitate the synthesis of versatile monomers using PGA as a raw material for the first time. Considering the enormous scope of commercial epoxides, this strategy also holds the promise of producing fused lactones with very large potential structural adjustability.

Synthesis and characterization of copolyesters

With the monomers in hand, we next studied their bulk copolymerization with ε-CL in the presence of stannous octanoate ($Sn(Oct)_2$) as the catalyst and 1,4-benzenedimethanol (BDM) as the initiator (Table 1), where $Sn(Oct)_2$ was chosen because of its wide compatibility in ROP and copolymerization of cyclic esters.[45–49] At first, as a control experiment, all fused monomers were discovered to show negligible conversions during homopolymerization catalyzed by $Sn(Oct)_2$ (Table S1). Then, we parallelly conducted the copolymerization of 6-MDO and ε-CL at different temperatures (80 °C, 100 °C, 120 °C, and 140 °C, Table 1, entries 1–4). After each polymerization, ε-CL was discovered to be converted nearly quantitatively, mirroring its high polymerizability. Meanwhile, the ultimate conversions of 6-MDO reached more than 40% and the content of 6-MDO in the copolymers was 18–19 mol% for polymerizations at 80 °C, 100 °C and 120 °C (Table 1, entries 1–3). In addition, the time required for polymerization was dramatically reduced from 80 °C to 120 °C (from 32 h to 4 h), and relatively high number-average molecular weight (M_n) copolymers can still be achieved at 120 °C (48.5 kDa). However, further increasing polymerization temperature to 140 °C resulted in a decrease in the ultimate conversion of 6-MDO (29%) and M_n of the copolymer

Table 1 Results of copolymerization of monomers and ε-CL catalyzed by $Sn(Oct)_2$.[a]

Entry	Monomer	[I] : [Cat] : [M] : [ε-CL]	T (°C)	t (h)	Conv.[b] (%) (M/ε-CL)	$M_{incorp.}$[c] (mol%)	$M_{n,GPC}$[d] (kDa)	$Đ$[d]
1	6-MDO	1 : 1 : 100 : 200	80	32	49/94	19	51.7	1.36
2	6-MDO	1 : 1 : 100 : 200	100	8	42/95	18	41.1	1.39
3	6-MDO	1 : 1 : 100 : 200	120	4	40/98	18	48.5	1.34
4	6-MDO	1 : 1 : 100 : 200	140	1	29/98	15	36.2	1.43
5	6-MDO	1 : 1 : 100 : 100	120	2	28/95	22	23.3	1.34
6	6-MDO	1 : 1 : 200 : 100	120	4	21/95	28	19.4	1.39
7	6-EDO	1 : 1 : 100 : 200	120	4	24/97	10	39.3	1.34
8	6-AMDO	1 : 1 : 100 : 200	120	4	52/96	21	31.1	1.29
9	6-PhDO	1 : 1 : 100 : 200	120	4	61/96	28	39.8	1.31
10	6-MDO	1 : 1 : 100 : 1000	120	8	31/98	6	101.3	1.34
11	6-MDO	1 : 1 : 200 : 1000	120	8	41/97	8	103.9	1.31
12	6-MDO	1 : 1 : 300 : 1000	120	8	35/96	10	91.7	1.35
13	6-MDO	1 : 1 : 400 : 1000	120	8	48/97	14	95.4	1.41
14	6-MDO	1 : 1 : 500 : 1000	120	10	46/98	17	87.6	1.31
15	6-EDO	1 : 1 : 500 : 1000	120	12	27/98	9	84.8	1.32
16	6-AMDO	1 : 1 : 300 : 1500	120	24	68/95	11	92.4	1.36
17	6-PhDO	1 : 1 : 300 : 1500	120	24	71/98	10	93.1	1.40
18	ε-CL	1 : 1 : 0 : 1000	120	4	-/89	—	102.7	1.22

[a] Conditions: initiator (I) = BDM, bulk copolymerization. [b] Conversion of monomers and ε-CL measured by ^{1}H NMR spectra. [c] Measured by the ^{1}H NMR spectra of the purified copolymer. [d] Determined by GPC analysis (CH_2Cl_2) and calibrated against the polystyrene standard.

(36.2 kDa) as well as broader dispersity (1.43) (Table 1, entry 4). This may be attributed to the fact that the polymerization equilibrium of 6-MDO was shifted towards backbiting reaction at high temperature, leading to the frequent occurrence of transesterification and chain transfer reactions. By comprehensively considering catalytic activity, ultimate conversion of 6-MDO and the molecular weight of the obtained copolymer, we chose 120 °C as the optimal temperature for subsequent polymerizations. Then, we successfully adjusted the incorporation ratio of 6-MDO in the copolymer by changing the feeding molar ratio of [6-MDO]/[ε-CL] (Table 1, entries 5–6). As the feeding molar ratio of [6-MDO]/[ε-CL] increased from 100 : 200 to 100 : 100, 200 : 100, the content of 6-MDO in the polymer increased from 18 mol% to 22 mol% and 28 mol%, respectively. Apart from 6-MDO, the copolymerization of other monomers with ε-CL was also studied under the same polymerization conditions ([M]/[ε-CL] feed molar ratio of 100 : 200). After 4 h, ε-CL was nearly consumed in each polymerization. Besides, the conversion of 6-EDO was 24%, yielding P(6-EDO)-*co*-PCL (M_n = 39.3 kDa, $Đ$ = 1.34) with 10 mol% of 6-EDO (Table 1, entry 7). Meanwhile, the conversion of 6-AMDO was higher (52%), and the content of 6-AMDO in the obtained P(6-AMDO)-*co*-PCL (M_n = 31.1 kDa, $Đ$ = 1.29) was nearly doubled (21 mol%, Table 1, entry 8). Moreover, the conversion of 6-PhDO was the highest (61%), and P(6-PhDO)-*co*-PCL (M_n = 39.8 kDa, $Đ$ = 1.31) contained 28 mol% of 6-PhDO (Table 1, entry 9). Upon reducing the feed molar ratio of *M* to [*M*]/[ε-CL] = 40 : 200, the monomer incorporation in P(6-EDO)-*co*-PCL (M_n = 38.8 kDa, $Đ$ = 1.34), P(6-AMDO)-*co*-PCL (M_n = 30.1 kDa, $Đ$ = 1.38) and P(6-PhDO)-*co*-PCL (M_n = 32.1 kDa, $Đ$ = 1.53) can be tuned down to 6 mol%, 11 mol% and 13 mol%, while retaining similar MW (Table S2, entries 2–4).

To further obtain high-MW copolyesters with tunable compositions, we conducted copolymerizations under the established polymerization protocol with higher monomer molar ratios ([6-MDO]/[ε-CL] ranging from 100 : 1000 to 500 : 1000). And we successfully produced high-MW P(6-MDO)-*co*-PCL (M_n ~87.6–103.9 kDa, $Đ$ ~1.31–1.41) with variable 6-MDO incorporation ratios ranging from 6 mol% to 17 mol% (Table 1, entries 10–14). Similarly, the copolymerization of other monomers with ε-CL also successfully produced high-MW copolyesters with tunable incorporation ratios. By fine-tuning the feeding ratio, we were able to synthesize P(6-EDO)-*co*-PCL, P(6-AMDO)-*co*-PCL, P(6-PhDO)-*co*-PCL with similar high MW, dispersity (M_n ~84.8–93.1 kDa, $Đ$ ~1.32–1.40) and comonomer content (10 mol%) (Table 1, entries 15–17).

To illuminate the copolymerization process in depth, we conducted a kinetic study on the copolymerization of ε-CL and 6-MDO. The crude mixture was probed by ^{1}H NMR analysis sequentially, and the conversion of each comonomer was plotted against reaction time. During the whole period of copolymerization, ε-CL and 6-MDO were converted simultaneously. Meanwhile, the conversion rate for ε-CL was apparently faster than 6-MDO: for example, after 1 h, the conversion of ε-CL was 82% whereas the conversion of 6-MDO was 28%. Upon further extending the reaction time to 3.5 h, the conversion of ε-CL was 97% and the ultimate conversion of 6-MDO reached 39% to produce the final random copolymer (Fig. 1A)

The structure of copolyester was further verified by the ^{1}H NMR spectrum (Fig. 1B and S11–S17). Within 4.15–3.95 ppm, the peaks belonging to ε-CL units (the methylene group proximal to the oxygen atom of ε-CL units) appeared as two sets of triplet signals, corresponding to CL-6-MDO heterosequence and CL–CL homosequence. Whereas only one set of singlet signal was observed for 6-MDO units (the methylene protons near the carbonyl group of 6-MDO units). This result further confirms that the copolyesters are mainly composed of repeating CL–CL units on the backbone with randomly incorporated 6-MDO units. Furthermore, the DOSY NMR spectrum of P(6-MDO)-*co*-PCL (Fig. 1C) gave only a single diffusion coefficient, confirming that the polymer is solely comprised of random copolyester rather than a physical blend of PCL and P(6-MDO). The ^{1}H and DOSY NMR spectra of all other copolymers also showed similar structural evidence of copolyesters (Fig. S12, S14, S16 and S18–S20).

To further analyze the microstructure of copolymers, 2D heteronuclear multiple bond correlation (HMBC) NMR was conducted for the obtained copolyesters (Fig. 2A and S21–24). The ^3J long–range correlation between the methylene proton signal at 4.08–4.03 ppm [–CH_2OC(O)–, H6] and the carbonyl carbon at 173.4 ppm [–CH_2OC(O)CH_2CH_2–, C1] corresponded to CL–CL homosequences. And the ^3J long–range correlation between the methylene proton at 4.16–4.12 ppm [–CH_2OC(O)–, H6′] and the

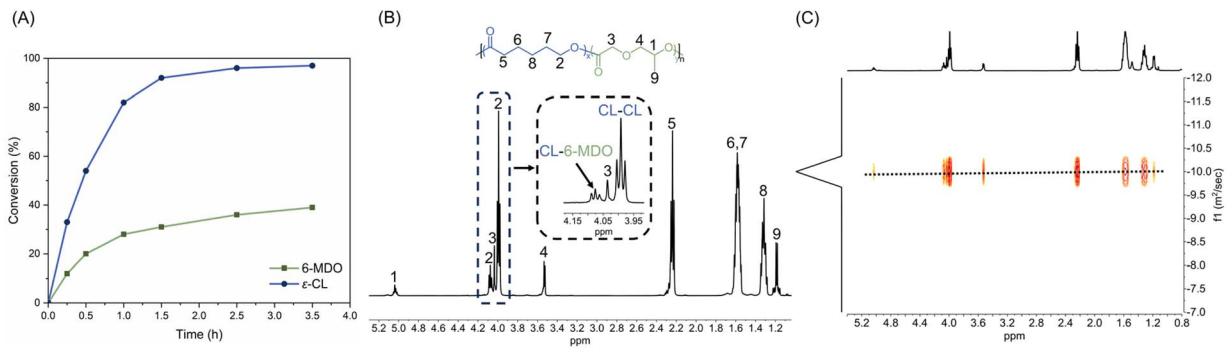

Fig. 1 (A) Monomer conversion as a function of time for the copolymerization of 6-MDO and ε-CL. (B) ^{1}H NMR spectra of P(6-MDO)-*co*-PCL (Table 1, entry 3). (C) A typical DOSY NMR spectrum of P(6-MDO)-*co*-PCL (Table 1, entry 3).

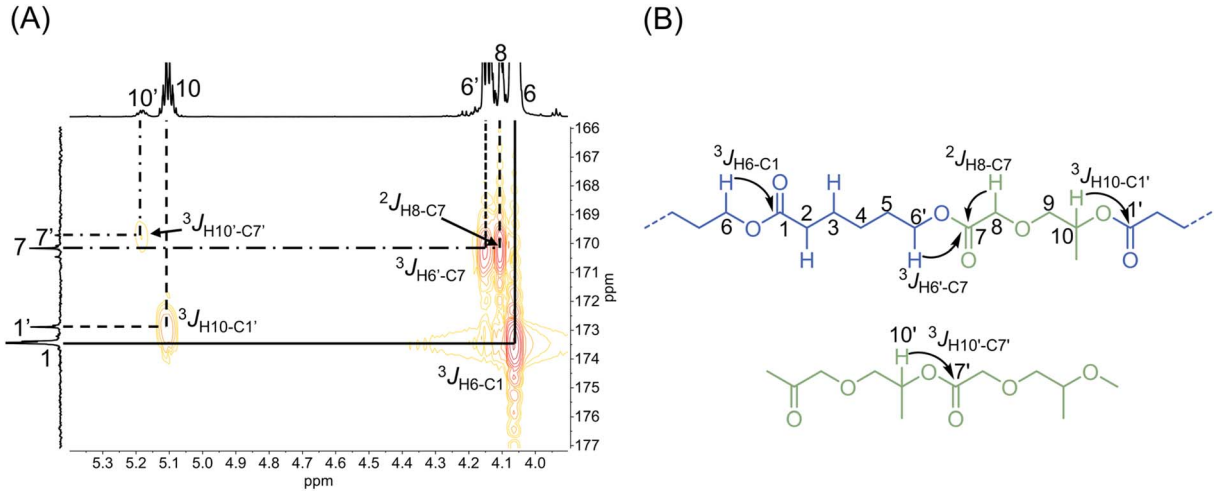

Fig. 2 (A) Selected regions from the 2D HMBC NMR spectra of P(6-MDO)-*co*-PCL (Table 1, entry 3). (B) Schematic representations of the relative correlations observed in P(6-MDO)-*co*-PCL (Table 1, entry 3).

carbonyl carbon at 170.1 ppm [–$CH_2OC(O)CH_2O$–, C7] corresponded to the CL-6-MDO heterosequences. Besides, the ^3J long–range correlation between the methine proton at 5.14–5.06 ppm [–$CH_2CH(CH_3)OC(O)CH_2CH_2$–, H10] and the carbonyl carbon at 172.9 ppm [–$CH_2CH(CH_3)OC(O)CH_2CH_2$–, C1′] corresponded to 6-MDO-CL heterosequences. The weak ^3J long–range correlation signal of the methine proton at 5.20–5.15 ppm [–$CH_2CH(CH_3)OC(O)CH_2CH_2$–, H10′] with carbonyl carbon at 169.7 ppm [–$CH_2CH(CH_3)OC(O)CH_2O$–, C7′] was attributed to 6-MDO-6-MDO homosequences, indicating the presence of trace consecutive 6-MDO units along the polymer chains. Therefore, the copolymer microstructure was inferred to consist of PCL chain segments containing randomly distributed and discrete monomer units, as well as trace repeating fused monomer segments.

To confirm the well-defined structure of the obtained copolyesters, we further conducted MALDI-TOF mass spectrometry on a low-MW copolyester (Fig. S26). The m/z values can be rationalized as a function of x and y: m/z = 114.14x+130.14y+138 (BDM) + 23 (Na^+), where x and y are the degrees of polymerization of ε-CL and 6-EDO, respectively. Therefore, the peaks in the spectrum can be assigned as a series of P(6-EDO)-*co*-PCL with different amounts of 6-EDO and ε-CL repeating units together with the BDM initiator.

Thermal properties and crystallinity of copolyesters

Then, we further studied the thermal and crystallization properties of high-MW copolyesters with a focus on illuminating their structure–property relationships. Thermal properties were evaluated by differential scanning calorimetry (DSC) and thermal gravimetric analysis (TGA) with copolymers of various compositions and similarly high MWs (84–100 kDa and $Đ$ of 1.3–1.4) (detailed data summarized in Table S3). Besides, a PCL homopolymer with M_n of 102.7 kDa was prepared and used for comparison (Table 1, entry 9).

As revealed by the curves of DSC (Fig. 3A and S43–45), all the copolymers displayed a melting peak in the second DSC heating run, indicating their semicrystalline nature. By increasing the content of 6-MDO from 6 mol% to 17 mol%, the melting point (T_m) of the copolymer decreased from 51.8 °C to 36.1 °C, validating that the disorder of polymer chains increased with the increase of 6-MDO incorporation. It is interesting to note that there was a linear correlation between T_m and the amount of ε-CL (mol%) (Fig. 3B), implying the precise tunability of the copolymer's primary structure over thermal properties. Meanwhile, the T_ms of P(6-MDO)$_{10}$-*co*-PCL$_{90}$, P(6-EDO)$_9$-*co*-PCL$_{91}$ and P(6-AMDO)$_{11}$-*co*-PCL$_{89}$ were similar (between 43.1 and 44.8 °C), which was attributed to the flexibility of the side groups that had little effect on the crystallization properties of the copolymers. However, the T_m of P(6-PhDO)$_{10}$-*co*-PCL$_{90}$ dropped to 35.6 °C, possibly because the bulky side phenyl group hampered the packing and neat arrangement of polymer chains and retarded the crystallization of the copolymer.

According to the TGA results (Fig. 3C), compared with pure PCL (decomposition temperature at 5% weight loss ($T_{d,5\%}$) = 333.6 °C), the incorporation of monomers resulted in a slight increase in $T_{d,5\%}$s for all copolymers: copolymers with increased amount of 6-MDO (from 6 mol% to 17 mol%) showed a slight decrease of $T_{d,5\%}$ from 345.2 to 333.9 °C. Besides, all copolymers showed good thermal stability with a $T_{d,5\%}$ of 333.8–345.2 °C (Fig. S52–S54) except for P(6-PhDO)$_{10}$-*co*-PCL$_{90}$, which show a decrease in $T_{d,5\%}$ to 316.7 °C.

We further studied the crystallinity of copolyesters with X-ray diffraction (XRD) analysis. It could be observed that the position of the diffraction peak for the copolymers remained unchanged in the case of copolymers with increased 6-MDO content (Fig. 3D) or copolymers composed of ε-CL and other comonomers (Fig. S56–S59), which were basically the same as the diffraction peak position of PCL. It is therefore inferred that all copolymer samples crystallize as an orthorhombic lattice, the same as PCL.

Mechanical properties of copolyesters

To explore the mechanical performance of these high-MW copolyesters and reveal the influence of copolymer

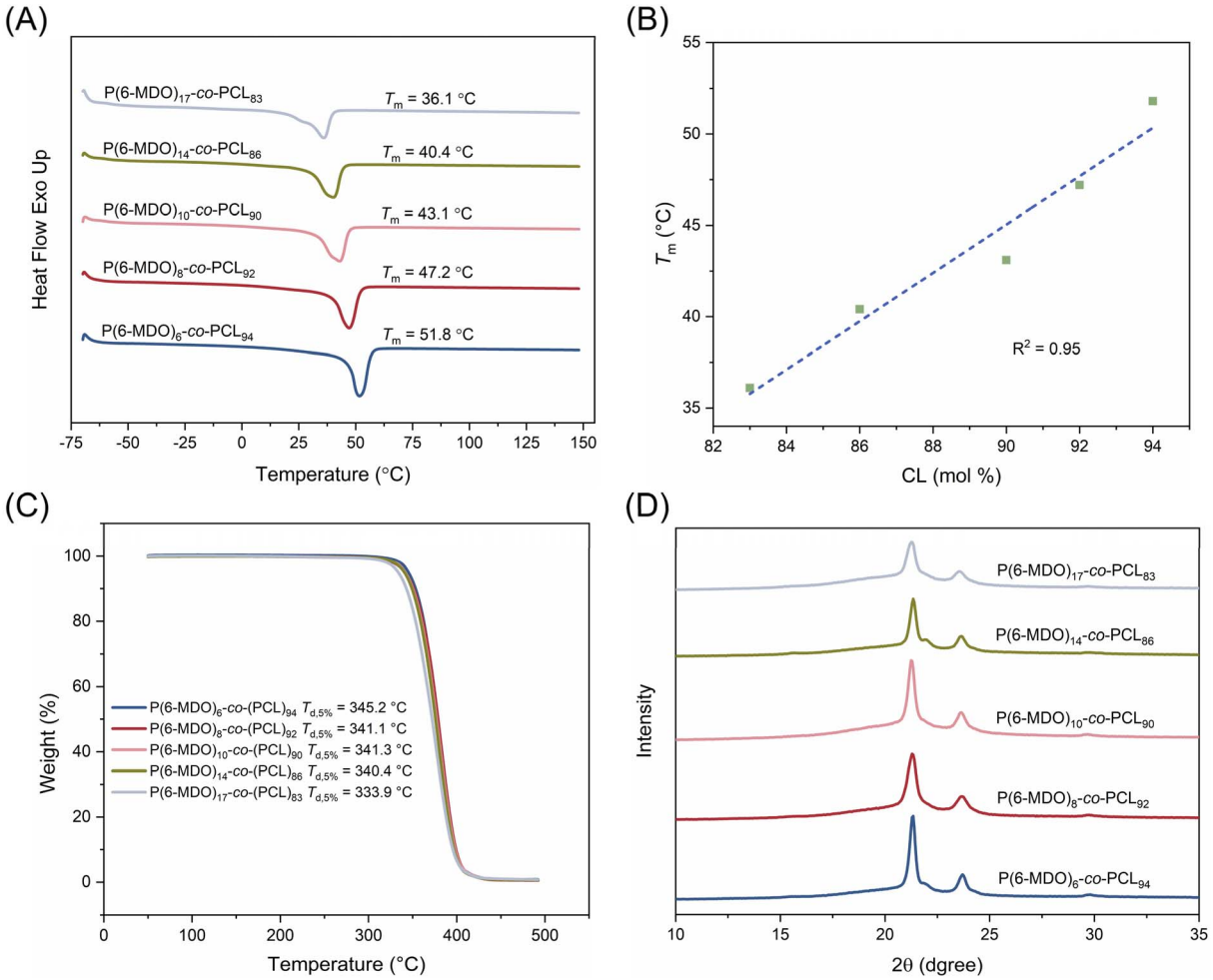

Fig. 3 (A) DSC traces of P(6-MDO)-*co*-PCL with varied 6-MDO incorporations (6–17 mol%). (B) Plot of the melting temperature (T_m) *vs.* the composition. (C) TGA traces of P(6-MDO)-*co*-PCL with varied 6-MDO incorporations (6–17 mol%). (D) XRD traces of P(6-MDO)-*co*-PCL with varied 6-MDO incorporations (6–17 mol%).

microstructure as well as composition on the polymers' mechanical properties, we conducted tensile tests on high-MW copolyesters (Table 1, entries 10–18). The mechanical test results are summarized in Table 2.

Compared to PCL, copolyesters with <10 mol% incorporated 6-MDO showed significantly improved tensile strength and ductility: P(6-MDO)$_6$-*co*-PCL$_{94}$ and P(6-MDO)$_8$-*co*-PCL$_{92}$ exhibited higher ultimate breaking tensile strength (σ_B) of up to 46.2 MPa with elongation at break (ε_B) of 1938–2186%. As a reference, the homopolymer of PCL displayed a σ_B of 36.7 ± 1.2 MPa and ε_B of 1464 ± 13% (Table 2, entry 9). Moreover, the mechanical performance of P(6-MDO)$_6$-*co*-PCL$_{94}$ and P(6-MDO)$_8$-*co*-PCL$_{92}$ was also superior to low-density polyethylene (LDPE, melt-flow index = 7.5) in terms of ultimate strength and ductility (σ_B = 12.0 ± 0.8 MPa and ε_B = 385 ± 21%).[50] Further increasing the content of 6-MDO in the random copolymer contributed to a reduction in tensile strength but a dramatic enhancement in ductility. P(6-MDO)$_{10}$-*co*-PCL$_{90}$ displayed reduced tensile strength (σ_B = 33.5 ± 0.8 MPa) but enhanced ductility (ε_B = 2209 ± 75%). And further increasing the 6-MDO content to 14 mol% led to a boost in elongation to 2661 ± 58% for P(6-MDO)$_{14}$-*co*-PCL$_{86}$ with a decreased σ_B of 31.0 ± 0.6 MPa. The copolymer with the maximum 6-MDO incorporation (17 mol%, P(6-MDO)$_{17}$-*co*-PCL$_{83}$) possessed the lowest σ_B of 27.1 ± 0.3 MPa but the highest stretchability of 2803 ± 26%. In addition, the modulus decreased gradually from 211 MPa to 65 MPa as the content of 6-MDO increased. While homo-PCL generally exhibited unvaried crystallinity during orientation due to the lack of chain mobility, PCL incorporated with a minor amount of 6-MDO may have higher segmental mobility of polymer chains, so as to foster the strain-induced crystallization of copolyesters during the tensile test. In this way, both tensile strength and stretchability would be dramatically enhanced. As the content of 6-MDO exceeded 10 mol%, the CL segment lengths in the polymer chains would be reduced. This in turn resulted in disrupted crystallization of copolymers and decreased tensile strength but continuously improved ductility. Notably, P(6-MDO)$_{14}$-*co*-PCL$_{86}$ exhibited the characteristics of an elastomer. To further evaluate the properties of elastomers, P(6-MDO)$_{14}$-*co*-PCL$_{86}$ was subjected to 10 reciprocating tensile

Table 2 Mechanical properties of the copolyesters and PCL

Entry	Sample	M_n (kDa)	$Đ$	σ_y (MPa)	σ_B (MPa)	ε_B (%)	E (MPa)
1	P(6-MDO)$_6$-*co*-PCL$_{94}$	101.3	1.34	12.6 ± 0.2	46.2 ± 2.8	1938 ± 51	211 ± 8
2	P(6-MDO)$_8$-*co*-PCL$_{92}$	103.9	1.31	10.0 ± 0.1	45.4 ± 0.3	2186 ± 91	162 ± 2
3	P(6-MDO)$_{10}$-*co*-PCL$_{90}$	91.7	1.35	7.8 ± 0.1	33.5 ± 0.8	2209 ± 75	86.3 ± 8.9
4	P(6-MDO)$_{14}$-*co*-PCL$_{86}$	95.4	1.41	5.7 ± 0.4	31.0 ± 0.6	2661 ± 58	54.9 ± 2.2
5	P(6-MDO)$_{17}$-*co*-PCL$_{83}$	87.6	1.31	5.6 ± 0.1	27.1 ± 0.3	2803 ± 26	65.4 ± 2.9
6	P(6-EDO)$_9$-*co*-PCL$_{91}$	84.8	1.32	7.9 ± 0.3	36.3 ± 0.1	2434 ± 36	98.9 ± 2.6
7	P(6-AMDO)$_{11}$-*co*-PCL$_{89}$	92.4	1.36	6.9 ± 0.3	32.3 ± 1.7	2097 ± 77	93.9 ± 7.9
8	P(6-PhDO)$_{10}$-*co*-PCL$_{90}$	93.1	1.40	4.2 ± 0.2	21.8 ± 1.0	2049 ± 47	73.7 ± 3.9
9	PCL	102.7	1.22	17.3 ± 0.4	36.7 ± 1.2	1464 ± 13	250 ± 13

tests where the sample was stretched to 100% strain and relaxed. Obvious plastic deformation and strain softening were observed in the first cycle, probably due to stress-induced polymer chain disentanglement. However, the plastic deformation produced in the first cycle was overcome, and the almost identical elastic behavior was maintained in the subsequent 2–10 cycles, with elastic recovery of 74–96% (Fig. 4B).

Subsequently, we investigated the mechanical properties of copolymers derived from other comonomers and ε-CL with similar high-MW and incorporation ratios (~10 mol%). Among the copolymers, P(6-EDO)$_9$-*co*-PCL$_{91}$ possessed the highest σ_B of 36.3 ± 0.1 MPa and the highest ε_B of 2434 ± 36%. Furthermore, P(6-MDO)$_{10}$-*co*-PCL$_{90}$ showed slightly lower tensile strength (σ_B = 33.5 ± 0.8 MPa) and ductility (ε_B = 2209 ± 75%). In addition, P(6-AMDO)$_{11}$-*co*-PCL$_{89}$ and P(6-PhDO)$_{10}$-*co*-PCL$_{90}$ showed comparable stretchability of 2097 ± 77% and 2049 ± 47%, but the tensile strength (σ_B = 32.3 ± 1.7 MPa) of P(6-AMDO)$_{11}$-*co*-PCL$_{89}$ was superior to that of P(6-PhDO)$_{10}$-*co*-PCL$_{90}$ (σ_B = 21.8 ± 1.0 MPa). Compared with poly(butylene adipate-*co*-terephthalate) (PBAT, Biocosafe 2003, T_m = 120 °C, σ_B = 16.4 ± 0.8 MPa, ε_B = 503 ± 47%, E = 64.2 ± 3.1 MPa),[51] the four copolymers exhibited higher tensile strength, ductility and modulus. For copolymers synthesized from 6-EDO, the ethyl side group can promote the regular arrangement and dense stacking of the polymer chains, due to its low conformational degree of freedom.[52] Meanwhile, it would also increase the flexibility of copolymers by breaking the integrity of crystallization. In this way, P(6-EDO)$_9$-*co*-PCL$_{91}$ displays better tensile strength and ductility than P(6-MDO)$_{10}$-*co*-PCL$_{90}$. Besides, because allyloxymethyl has larger steric hindrance than that of methyl and ethyl but is more flexible than the phenyl group at the same time, the polymer chains of P(6-AMDO)$_{11}$-*co*-PCL$_{89}$ are more prone to regular stacking than P(6-PhDO)$_{10}$-*co*-PCL$_{90}$, resulting in higher tensile strength for P(6-AMDO)$_{11}$-*co*-PCL$_{89}$ than P(6-PhDO)$_{10}$-*co*-PCL$_{90}$.

Chemical recycling of copolyesters

Chemical recycling of polymers to monomers is a desirable strategy for achieving a circular plastic economy. In view of the success of the closed-loop recovery of homopolymers such as P(6-MDO) and PCL,[31,33,53] we believe that copolymers also have the potential for closed-loop recovery. First, we studied the depolymerization of copolymers by treating them with commonly adopted commercially available Lewis acid $MgCl_2$ as a catalyst at 230 °C for 5 h. However, the catalyst furnished modest depolymerization conversions (79–87% of fused monomers and 13–23% of ε-CL) for P(6-MDO)$_{18}$-*co*-PCL$_{82}$ (M_n = 48.5 kDa, $Đ$ = 1.34), P(6-EDO)$_{10}$-*co*-PCL$_{90}$ (M_n = 39.3 kDa, $Đ$ = 1.34) and P(6-AMDO)$_{21}$-*co*-PCL$_{79}$ (M_n = 31.1 kDa, $Đ$ = 1.29), and low conversion (~0% of fused monomers and 7% of ε-CL) for P(6-PhDO)$_{28}$-*co*-PCL$_{72}$ (M_n = 39.8 kDa, $Đ$ = 1.31) (Table S13). In order to improve the recovery of copolymers, the copolymers were treated with another yttrium catalyst (Y(CH$_2$SiMe$_3$)$_3$(-THF)$_2$, 5 wt%) at 230 °C for 5 h. Excitingly, the utilization of the new catalyst resulted in satisfactory recovery for each monomer (98–99% of fused monomers and 87–91% of ε-CL) (Table S14, Fig. 5). Thereby, we successfully recycled these copolymers back

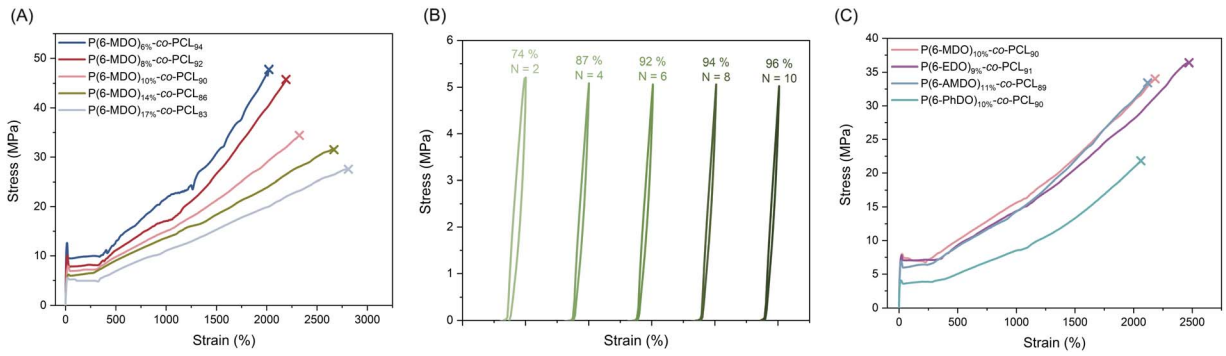

Fig. 4 (A) Stress–strain curves of P(6-MDO)-*co*-PCL with varied 6-MDO incorporations (6–17 mol%). (B) Cyclic tensile testing for P(6-MDO)$_{14}$-*co*-PCL$_{86}$. (C) Stress–strain curves of copolymers with different substituent monomers.

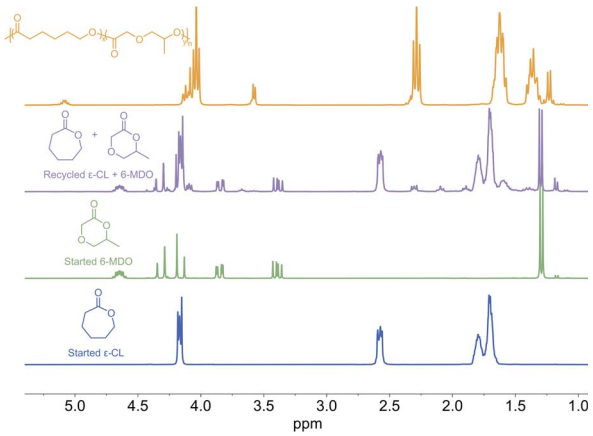

Fig. 5 Overlay of the ^{1}H NMR spectrum of P(6-MDO)-*co*-PCL, recycled ε-CL and 6-MDO, and started monomer 6-MDO and ε-CL for comparison.

to monomers in an efficient manner using the appropriate catalyst $Y(CH_2SiMe_3)_3(THF)_2$, establishing a monomer–polymer–monomer closed-loop life cycle.

Conclusions

In conclusion, we have achieved the upcycling of PGA into fused lactones using epoxides under mild conditions for the first time, allowing for the selection of different epoxides to achieve versatile modulation of monomers. And then simple one-pot bulk copolymerization of ε-CL and monomers was used to synthesize high-MW copolymers with 6-MDO incorporation of 6–17 mol% and incorporation of different substituent monomers of around 10 mol%. The properties of all copolymers were characterized to analyze the effects of monomer incorporation and monomer substituents on the properties of copolymers. All copolymers are semi-crystalline polymers with good thermal stability ($T_{d,\ 5\%}$ > 316 °C). Compared to homopolymer PCL, the T_ms of copolymers were lower. The 6-MDO units made the polymer chains disordered, which led to the decrease of T_m with the increase of 6-MDO incorporation. The bulky substituent phenyl group of 6-PhDO hindered the perfect packing of the polymer chain segments in the crystalline lattice, resulting in a decrease in the T_m of the copolymer to 35.6 °C.

When the incorporation amount of 6-MDO was less than 10 mol%, the tensile strength (45.4–46.2 MPa) and ductility (1938–2186%) of the copolymers were significantly improved in comparison to PCL. Further increasing the content of 6-MDO in the copolymer contributed to a dramatic enhancement in the material ductility but reduced tensile strength. Among them, P(6-MDO)$_{14}$-*co*-PCL$_{86}$ exhibited the features of an elastomer, with elastic recovery of 74–96%. When comparing the mechanical properties of copolymers with the incorporation of different substituent monomers of around 10 mol%, among the four copolymers, P(6-EDO)$_9$-*co*-PCL$_{91}$, owing to the low conformational degree of freedom of ethyl, displayed the highest σ_B of up to 36.3 ± 0.1 MPa, with the highest stretchability of 2434 ± 36%. The largest steric hindrance of phenyl caused a decrease in tensile strength (σ_B = 21.8 ± 1.0 MPa) of P(6-PhDO)$_{10}$-*co*-PCL$_{90}$ while maintaining high ductility (ε_B = 2049 ± 47%). All copolymers demonstrated a wider range of thermal properties and mechanical performances depending on their compositions and monomer substituents. And these copolymers could be efficiently closed-loop depolymerized into initial monomers, establishing a closed-loop life cycle for a sustainable circular polymer economy.

Author contributions

Feng Ren: investigation, data curation, visualization, writing of the original draft. Zhuangzhuang Liang: investigation, data curation. Yifan Jia: data curation. Bokun Li: data curation. Zhiqiang Sun, funding acquisition, manuscript review and editing. Chenyang Hu: conceptualization, funding acquisition, manuscript review and editing. Xuan Pang: funding acquisition, supervision, manuscript review and editing. Xuesi Chen: supervision.

Conflicts of interest

There are no conflicts to declare.

Data availability

The data supporting this article have been included as part of the SI.

Supplementary information: experimental procedures and detailed characterization of monomers and copolyesters. See DOI: https://doi.org/10.1039/d5sc05815e.

Acknowledgements

This work was financially supported by the National Natural Science Foundation of China, Fund for Distinguished Young Scholars (No. 52325301), the CAS Project for Young Scientists in Basic Research (No. YSBR-094), the Science and Technology Development Plan of Jilin Province-Provincial Natural Science Foundation of Jilin (SKL202302035), and the National Natural Science Foundation of China (No. 22293062 and 52203017). We thank Prof. Bo Liu (Changchun Institute of Applied Chemistry, Chinese Academy of Sciences) for kindly offering the $Y(CH_2SiMe_3)_3(THF)_2$ catalyst.

Notes and references

1 C. V. Aarsen, A. Liguori, R. Mattsson, M. H. Sipponen and M. Hakkarainen, *Chem. Rev.*, 2024, **124**, 8473–8515.
2 C. Shi, E. C. Quinn, W. T. Diment and E. Y. X. Chen, *Chem. Rev.*, 2024, **124**, 4393–4478.
3 M. Hong and E. Y. X. Chen, *Green Chem.*, 2017, **19**, 3692–3706.
4 G. Xu and Q. Wang, *Green Chem.*, 2022, **24**, 2321–2346.
5 F. M. Haque, J. S. A. Ishibashi, C. A. L. Lidston, H. Shao, F. S. Bates, A. B. Chang, G. W. Coates, C. J. Cramer, P. J. Dauenhauer, W. R. Dichtel, C. J. Ellison, E. A. Gormong, L. S. Hamachi, T. R. Hoye, M. Jin,

J. A. Kalow, H. J. Kim, G. Kumar, C. J. LaSalle, S. Liffland, B. M. Lipinski, Y. Pang, R. Parveen, X. Peng, Y. Popowski, E. A. Prebihalo, Y. Reddi, T. M. Reineke, D. T. Sheppard, J. L. Swartz, W. B. Tolman, B. Vlaisavljevich, J. Wissinger, S. Xu and M. A. Hillmyer, *Chem. Rev.*, 2022, **122**, 6322–6373.

6 Y. Xia, C. Zhang, Y. Wang, S. Liu and X. Zhang, *Chin. Chem. Lett.*, 2024, **35**, 108860.

7 X. Zhao, X. Wu, Q. Wang and F. Wu, *Science*, 2025, **388**, 1034.

8 B. Sun, J. Zhang, M. Wang, S. Yu, Y. Xu, S. Tian, Z. Gao, D. Xiao, G. Liu, W. Zhou, M. Wang and D. Ma, *Nat. Sustain.*, 2023, **6**, 712–719.

9 W. Xiong and H. Lu, *Sci. China: Chem.*, 2023, **33**, 725–738.

10 Y. Jia, B. Li, Y. Sun, C. Hu, X. Li, S. Liu, X. Wang, X. Pang and X. Chen, *Chem Bio Eng.*, 2024, **1**, 559–567.

11 N. Ashammakhi and P. Rokkanen, *Biomaterials*, 1997, **18**, 3–9.

12 P. K. Samantaray, A. Little, D. M. Haddleton, T. McNally, B. Tan, Z. Sun, W. Huang, Y. Ji and C. Wan, *Green Chem.*, 2020, **22**, 4055–4081.

13 O. D. Cabaret, B. M. Vaca and D. Bourissou, *Chem. Rev.*, 2004, **104**, 6147–6176.

14 Y. Lu, J. H. Swisher, T. Y. Meyer and G. W. Coates, *J. Am. Chem. Soc.*, 2021, **143**, 4119–4124.

15 M. Rabnawaz, I. Wyman, R. Auras and S. Cheng, *Green Chem.*, 2017, **19**, 4737–4753.

16 *Polyglycolic Acid Market Size, Share, Growth, and Industry Analysis, By Types (Industrial Grade, Medical Grade), By Applications Covered (Oil and Gas Industry, Medical Industry, Packing Industry, Others), Regional Insights and Forecast to 2033*, **https://www.globalgrowthinsights.com/market-reports/polyglycolic-acid-market-113122**, (accessed 2025).

17 S. Shawe, F. Buchanan, E. Harkin-Jones and D. Farrar, *J. Mater. Sci.*, 2006, **41**, 4832–4838.

18 X. Hu, G. Hu, K. Crawford and C. B. Gorman, *J. Polym. Sci., Part A: Polym. Chem.*, 2013, **51**, 4643–4649.

19 Y. Fu, L. Zhu, B. Liu, X. Zhang and Y. Weng, *Polymer*, 2024, **307**, 127295.

20 K. Saigusa, H. Saijo, M. Yamazaki, W. Takarada and T. Kikutani, *Polym. Degrad. Stab.*, 2020, **172**, 109054.

21 M. Ayyoob, D. H. Lee, J. H. Kim, S. W. Nam and Y. J. Kim, *Fibers Polym.*, 2017, **18**, 407–415.

22 X. Zhou, M. Zha, J. Cao, H. Yan, X. Feng, D. Chen and C. Yang, *ACS Sustain. Chem. Eng.*, 2021, **9**, 10948–10962.

23 N. K. Kang, M. Kim, K. Baek, Y. K. Chang, D. R. Ort and Y.-S. Jin, *Chem. Eng. J.*, 2022, **433**, 133636.

24 E. Göktürk, A. G. Pemba and S. A. Miller, *Polym. Chem.*, 2015, **6**, 3918–3925.

25 S. Lee, C. Hongo and T. Nishino, *Macromolecules*, 2017, **50**, 5074–5079.

26 C. Schmidt, M. Behl, A. Lendlein and S. Beuermann, *RSC Adv.*, 2014, **4**, 35099–35105.

27 V. Sanko, I. Sahin, U. Aydemir Sezer and S. Sezer, *Polym. J.*, 2019, **51**, 637–647.

28 P. Zhang, R. Yang, Y. Wang, H. Sun, G. Xu and Q. Wang, *Polymer*, 2025, 317.

29 P. Zhang, V. Ladelta and N. Hadjichristidis, *J. Am. Chem. Soc.*, 2023, **145**, 14756–14765.

30 X. Liu, M. Hong, L. Falivene, L. Cavallo and E. Y. X. Chen, *Macromolecules*, 2019, **52**, 4570–4578.

31 F. Ren, Z.-Z. Liang, M.-X. Niu, C.-Y. Hu and X. Pang, *Chin. J. Polym. Sci.*, 2023, **42**, 168–175.

32 H.-Y. Huang, M. Xie, S.-Q. Wang, Y.-T. Huang, Y.-H. Luo, D.-G. Yu, Z. Cai and J.-B. Zhu, *J. Am. Chem. Soc.*, 2025, **147**, 7788–7798.

33 W. Zhao, Z. Guo, J. He and Y. Zhang, *Angew. Chem., Int. Ed.*, 2025, **64**, e202420688.

34 W.-M. Ren, H.-J. Gao and T.-J. Yue, *Chin. J. Polym. Sci.*, 2021, **39**, 1013–1019.

35 S.-H. Pyo, J. H. Park, V. Srebny and R. Hatti-Kaul, *Green Chem.*, 2020, **22**, 4450–4455.

36 L. S. Nair and C. T. Laurencin, *Prog. Polym. Sci.*, 2007, **32**, 762–798.

37 D. Bandelli, C. Helbing, C. Weber, M. Seifert, I. Muljajew, K. D. Jandt and U. S. Schubert, *Macromolecules*, 2018, **51**, 5567–5576.

38 M. Mader, V. Jérôme, R. Freitag, S. Agarwal and A. Greiner, *Biomacromolecules*, 2018, **19**, 1663–1673.

39 Y.-C. Jiang, X.-F. Wang, Y.-Y. Xu, Y.-H. Qiao, X. Guo, D.-F. Wang, Q. Li and L.-S. Turng, *Biomacromolecules*, 2018, **19**, 3747–3753.

40 M. A. Woodruff and D. W. Hutmacher, *Prog. Polym. Sci.*, 2010, **35**, 1217–1256.

41 G. Si, C. Li, M. Chen and C. Chen, *Angew. Chem., Int. Ed.*, 2023, **62**, e202311733.

42 B. Dong, G. Xu, R. Yang, X. Guo and Q. Wang, *Macromolecules*, 2023, **56**, 10143–10152.

43 X. Tang, C. Shi, Z. Zhang and E. Y. X. Chen, *Macromolecules*, 2021, **54**, 9401–9409.

44 C. Wischke, M. Löbler, A. T. Neffe, B. D. Hanh, M. Zierke, K. Sternberg, K. P. Schmitz, R. Guthoff and A. Lendlein, *Macromol. Symp.*, 2011, **309–310**, 59–67.

45 T. Fuoco and A. Finne-Wistrand, *Biomacromolecules*, 2019, **20**, 3171–3180.

46 H. R. Kricheldorf, I. K. Saunders and A. Stricker, *Macromolecules*, 2000, **33**, 702–709.

47 A. Kowalski, A. Duda and S. Penczek, *Macromolecules*, 2000, **33**, 689–695.

48 Z. Li, D. Zhao, Y. Shen and Z. Li, *Angew. Chem., Int. Ed.*, 2023, **62**, e202302101.

49 Z. Li, Y. Shen and Z. Li, *ACS Sustain. Chem. Eng.*, 2022, **10**, 8228–8238.

50 J.-J. Tian, R. Li, E. C. Quinn, J. Nam, E. R. Chokkapu, Z. Zhang, L. Zhou, R. R. Gowda and E. Y. X. Chen, *Nature*, 2025, **643**, 967–974.

51 X. Zhou, A. Mohanty and M. Misra, *J. Polym. Environ.*, 2013, **21**, 615–622.

52 C. De Rosa, M. Scoti, O. Ruiz de Ballesteros, R. Di Girolamo, F. Auriemma and A. Malafronte, *Macromolecules*, 2020, **53**, 4407–4421.

53 C. F. Gallin, W. W. Lee and J. A. Byers, *Angew. Chem., Int. Ed.*, 2023, **62**, e202303762.